A proposal for model-independent 3D wave field reconstruction from reflection data

Kees Wapenaar, Delft Univ. of Technology; Filippo Broggini and Roel Snieder, Colorado School of Mines*

SUMMARY

With seismic interferometry one can retrieve the response to a virtual source inside an unknown medium, assuming there is a receiver at the position of the virtual source. In a companion paper, Broggini et al. show that for the 1D situation the requirement of having an actual receiver inside the medium can be circumvented. They show that the virtual source response can be obtained from reflection data only. This paper is a first step towards the generalization of their method to the 3D situation. We show how the full response to a virtual source inside the medium can be obtained from the reflection response at the surface. We also indicate how this method can be used to handle internal multiple scattering in migration.

INTRODUCTION

Broggini et al. (2011) discuss the connection between seismic interferometry and inverse scattering. They show that there are different ways to reconstruct the wave field of a source in the interior of an unknown medium. (1) With seismic interferometry it is possible to retrieve the response to a virtual source inside the medium, assuming there is a receiver at the position where the virtual source is to be created and assuming the medium is surrounded by sources. The medium parameters need not be known. (2) With 1D inverse scattering the response to a virtual source inside the medium can be obtained when there are only reflected waves recorded at one side of the medium. In both approaches the virtual source response contains all scattering effects of the medium. Broggini et al. (2011) show that the second approach is possible for the 1D situation without knowing the medium parameters. This is very fascinating, because it allows one to obtain the same virtual source response as with seismic interferometry (including all scattering effects), but without the need of having receivers inside the medium. An essential element of their approach is to use a complicated incident wave that is designed to colllapse onto a point inside the medium at a specified time.

Broggini et al. (2011) suggest that their insights might be extended to three dimensions. This paper is a first step towards the generalization of their concepts to three dimensions. The method we propose here is not fully independent of knowledge about the medium. The proposed method requires the reflection response of the medium measured at the surface, supplemented with independent information about first arrivals, to reconstruct the full response to a virtual source inside the medium, including all scattering effects. We also indicate how this method can be extended to handle internal multiple scattering in migration in a stable way.

3D WAVE FIELD RECONSTRUCTION

Figure 1a shows an inhomogeneous lossless lower half-space ($z > 0$), illuminated from above by a complex downward propagating incident wave field[1]. This incident field starts with an acausal wave front (just above the upper red curve), followed by a complex coda (to be discussed below). For the moment we do not prescribe the spatial shape of the wave front. Figure 1b shows the reflected field, recorded at $z = 0$, and propagating upward into the upper half-space. The reflection response contains acausal and causal contributions. The red curves in these figures, which are symmetric around $t = 0$, separate the space-time domain into three distinct regions. (1) The acausal region above the upper red curve contains a downgoing wave front in Figure 1a and is zero in Figure 1b. (2) The region between the red curves contains downgoing (Figure 1a) and upgoing (Figure 1b) waves. (3) The causal region below the lower red curve contains upgoing waves in Figure 1b and is zero in Figure 1a.

From hereonward we assume that the coda of the incident field in Figure 1a is chosen such that, between the red curves, it is minus the time-reversed reflection response in Figure 1b. We discuss later how this can be achieved; for the moment we consider this as a given fact.

Figure 2a shows the superposition of the incident and reflected waves at $z = 0$. This total wave field obeys the wave equation in the inhomogeneous medium; Figure 2a is just a cross section of the total field at $z = 0$. Because the medium is assumed lossless, the time-reversed version of the total wave field is also a solution of the wave equation. Figure 2b shows a superposition of the total wave field and its time-reversed version. Because of the italicized assumption above, this superposition is zero between the red curves. Moreover, since time-reversal changes a downgoing field into an upgoing field and vice versa, the fields above and below the red curves in Figure 2b are downgoing and upgoing, respectively (at $z = 0$). Of course the superposition in Figure 2b is also a solution of the wave equation in the inhomogeneous medium.

Until this point we did not make any assumptions about the spatial shape of the wave front above the upper red curve in Figure 1a. Let us now define a virtual source somewhere in the subsurface. This can be a point source, a plane-wave source, or for example an extended source coinciding with a curved reflector. Figure 3a shows the situation of a virtual point source and the direct paths to the surface $z = 0$. Figure 3b shows the corresponding traveltime curve and the first arriving wave front. From hereonward we assume that the incident field in Figure 1a has been chosen such that the wave front above the upper red curve is the time-reversed version of the wave front in Figure 3b. This fixes the shape of the incident field in Figure 1a to a converging wave of which the first arrival focuses at $t = 0$ at the position of the virtual source.

More important is the interpretation of Figure 2b. First consider the causal part of the response in this figure (and recall that this is an upgoing field at $z = 0$). The first wave front just below the lower red curve is, by construction, the wave front coming directly from the virtual source in Figure 3a. We already noted that the response in Figure 2b is a solution of the wave equation. Hence, for consistency with the wave equation, the coda following the first arriving wave front must be caused by the scattering that the primary wave front encounters during propagation to the surface $z = 0$. Since the wave equation accounts for downward and upward propagation, this coda contains the waves reflected by scatterers above as well as below the virtual source, see Figure 4.

[1]The wave fields in Figures $1 - 3$ are not actual modeling results but cartoons, to illustrate the principle.

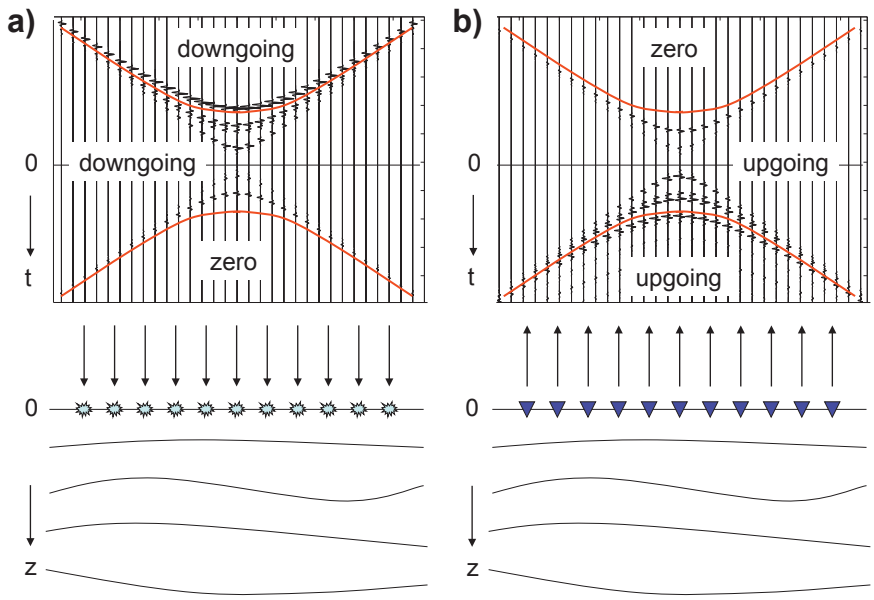

Fig. 1: *(a) Incident wave field at $z = 0$, consisting of an acausal wave front and a complex coda. (b) Reflected wave field. Between the red curves the coda of the incident field in (a) is minus the time-reversed reflected field in (b).*

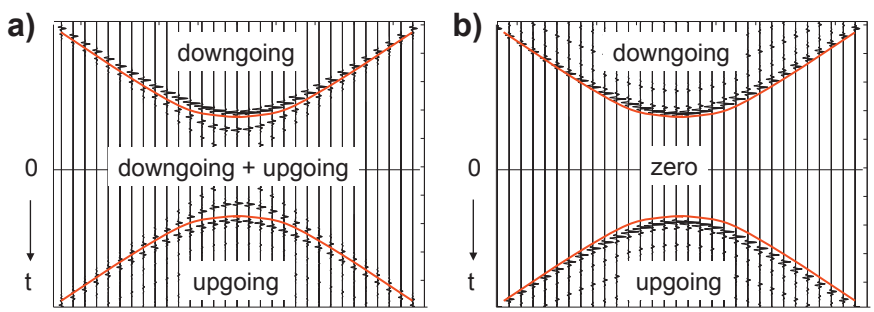

Fig. 2: *(a) Total wave field at $z = 0$ (superposition of Figures 1a and 1b). (b) Total wave field plus time-reversed version.*

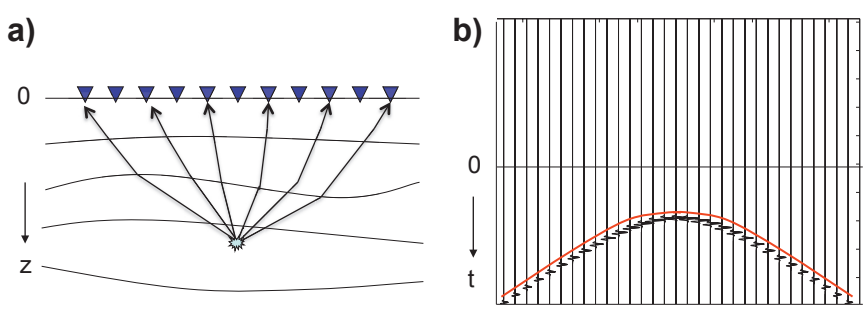

Fig. 3: *(a) Virtual source and direct paths. (b) Traveltime curve and direct arriving wave front.*

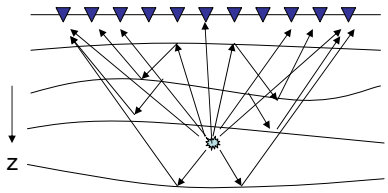

Fig. 4: *Virtual source with direct and all scattered paths. This model explains the causal part of the response in Figure 2b.*

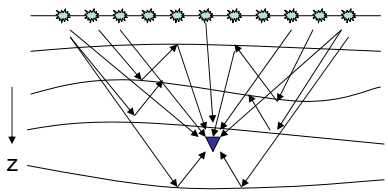

Fig. 5: *Virtual receiver. This is an alternative interpretation of the causal part of the response in Figure 2b.*

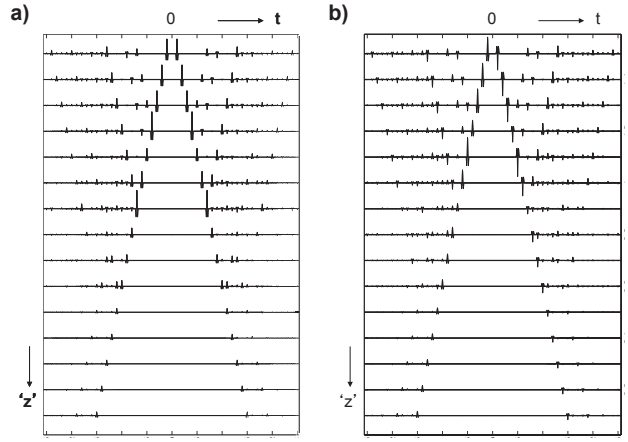

Fig. 6: *(a) Symmetric virtual receiver responses in a 1D medium. (b) Antisymmetric virtual receiver responses.*

How can there be a source in the lower half-space, given that the response in Figure 2b was constructed from the response of a source-free lower half-space? To see this, consider the acausal part of the response in Figure 2b. This is precisely the time-reversed version of the causal part. It is a cross section (at $z = 0$) of the acausal wave field in the lower half space. This acausal field converges and focuses at the position of the virtual source, after which it diverges, to give the causal wave field. Hence, for the total wave field in Figure 2b the lower half-space is indeed source-free; there is only focusing of waves at the position of the virtual source. Only when the causal part is considered in isolation, a singularity is required at the position of the virtual source to explain the causal response.

Note that the amplitude of the virtual source is as yet undetermined, because, by construction, the first arrival in the causal part in Figure 2b consists of the first arriving wave front in Figure 3b, plus a perturbation by the reflection response in Figure 1b just below the lower red curve.

Let us now see how the incident field in Figure 1a can be constructed in such a way that, between the red curves, its coda is minus the time-reversed reflection response in Figure 1b. For this we propose to use a 3D version of the iterative procedure of Rose (2002). The initial incident field is the time-reversal of the wave front in Figure 3a. This is fed into the medium and the response is measured at $z = 0$ (this can be accomplished by convolving the incident field with the reflection impulse responses (Green's functions) of the subsurface and summing over the sources). The part of the obtained reflection response between the red curves is reversed in time and *subtracted from* the initial incident field. The updated incident field is fed into the medium, etc. This procedure is expected to converge because in each iteration the reflected energy is smaller than the incident energy.

In summary, the procedure we discussed in this section yields the response to a virtual source (Figures 2b and 4), including correct internal multiple scattering, without needing a receiver at the position of the virtual source and without needing detailed knowledge of the medium. As input we need (1) the direct arriving wave front at the surface of a virtual source in the subsurface, and (2) the reflection impulse responses for all source and receiver positions at the surface. The direct arriving wave front can be obtained by modeling in a macro model or, when the virtual source is located at an interface, directly from the data by the CFP method (Berkhout, 1997). The required reflection impulse responses are obtained from seismic reflection data after surface-related multiple elimination (Verschuur et al., 1992) and deconvolution for the source wavelet.

Broggini et al. (2011) propose applications like full waveform inversion, subsalt imaging and, last but not least, focussing of energy to increase the fractures in a reservoir. In the next section we indicate how the method could be extended to properly handle internal multiples in prestack migration.

INTERNAL MULTIPLES IN MIGRATION

Consider again Figure 4, which shows the configuration that explains the created virtual source response in Figure 2b (i.e., the causal part of Figure 2b). Using source-receiver reciprocity, Figure 2b can also be interpreted as the response to sources at the surface, observed by a virtual downhole receiver, see Figure 5. If we repeat the procedure for many downhole receiver positions, we obtain the configuration that Bakulin and Calvert (2006) use as the starting point for their virtual source method (except that no actual downhole receivers are required to obtain Figure 2b). Hence, by crosscorrelating the obtained responses at different virtual receiver positions and summing over the sources at the surface, one obtains the redatumed response, with virtual sources and receivers in the subsurface. Snieder et al. (2006) show that such a redatumed response contains spurious multiples. To reduce the amount of spurious multiples, Mehta et al. (2007) propose to apply decomposition prior to correlation. The spurious multiples are (at least in theory) entirely removed by replacing the correlation by a multidimensional deconvolution (MDD) process (Wapenaar and van der Neut, 2010). Also MDD requires that the data at the downhole receivers are decomposed into downgoing and upgoing waves. Single-component data are not sufficient for this purpose, so let's see how we can generate a second type of data to enable decomposition.

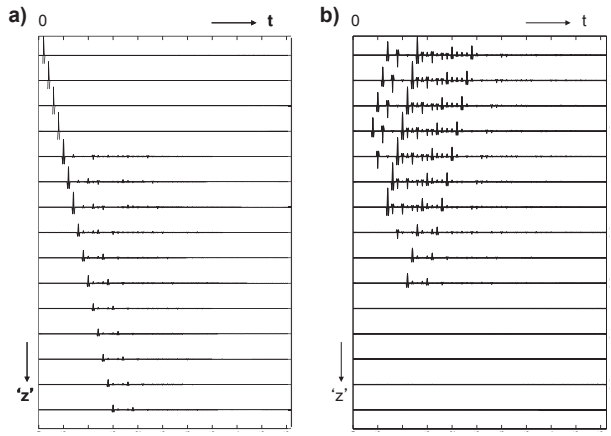

Fig. 7: *(a) Downgoing field. (b) Upgoing field.*

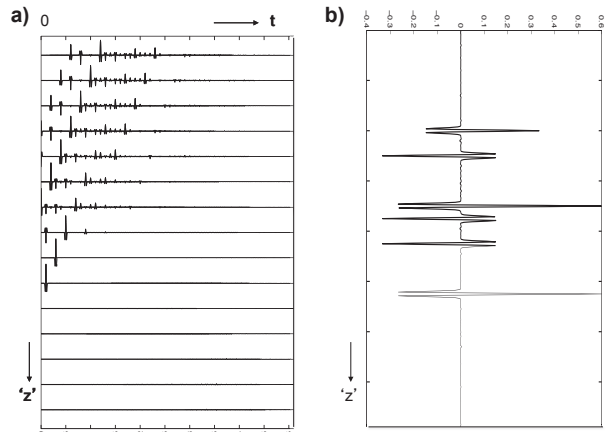

Fig. 8: *(a) Deconvolution result. (b) Image at $t = 0$.*

Our initial assumption was that between the red curves the coda of the incident field in Figure 1a is *minus* the time-reversed reflection response in Figure 1b. We now consider a second type of incident field of which the coda is *plus* the time-reversed reflection response between the red curves. This means that in the 3D version of the iterative procedure of Rose (2002), the words *"subtracted from"* should be replaced by *"added to"*. The new incident and reflected fields are superposed (like in Figure 2a). Next, the time-reversed version of this superposition is subtracted from it (instead of added to it). The result is similar as in Figure 2b, except that it is now antisymmetric in time. The new created virtual source (Figure 4) or virtual receiver (Figure 5) is therefore also antisymmetric (like a dipole). If we subtract the antisymmetric from the symmetric response, we obtain the downgoing field at the virtual receiver in Figure 5; if we add the two responses the upgoing field at the virtual receiver is obtained. Having obtained the downgoing and upgoing waves at the virtual receivers, we can continue by applying interferometry by MDD. This gives the virtual source response of the half-space below the virtual receivers, with the effect of the medium above the virtual receivers removed. Of course we can apply the whole procedure at any depth and hence obtain virtual source responses at any depth. Selecting the $t = 0$ component gives a migrated image, free of contamination by internal multiples. A more efficient procedure would be to generate virtual source responses at a finite number of depth levels and apply standard migration of these responses between these depth levels.

We illustrate this with a 1D example. Note that for the 1D situation we don't need any information about the medium (Broggini et al., 2011). We consider a horizontally layered medium with six layers and a half-space (propagation velocities 1000, 2000, 1000, 4000, 2000, 1000, 4000 m/s), and model the plane-wave reflection impulse response of this medium (not shown). We follow the 1D version of the wave field reconstruction procedure discussed in the previous section. For the 1D situation, each of the panels in Figures $1 - 3$ reduces to a single trace. The 1D equivalent of the symmetric response in Figure 2b is represented by one of the traces in Figure 6a. The other traces in Figure 6a represent virtual receiver responses at other depths. The label 'z' denotes pseudo-depth (actually it is one-way traveltime). Figure 6b represents the antisymmetric virtual receiver responses at all depths. Figures 7a and b are obtained by subtracting and adding, respectively, Figures 6a and b (only the causal parts are shown). The results are interpreted as the downgoing and upgoing wave fields at all depths. Figure 8a is obtained by deconvolving the upgoing field in Figure 7 by the downgoing field (and convolving the result with a wavelet). Each trace can be seen as a redatumed response, with the virtual source and receiver at the same depth and the effects of the overburden completely removed. Figure 8b is the cross-section of Figure 8a at $t = 0$ (obtained from a finer sampled version), convolved with a wavelet. This can be seen as a 1D migrated image, without contamination by internal multiples. The reflection coefficients perfectly match those of the layered model (not shown). The method is quite stable. Because it is non-recursive, each layer can be imaged separately, so the method does not suffer from error propagation. To emphasize this, the results in Figures $6 - 8$ were obtained by starting at the largest depth and subsequently imaging the shallower depths.

CONCLUSIONS

We proposed a first step towards the generalization of the model-independent wave field reconstruction method of Broggini et al. (2011) to three dimensions. Unlike the 1D method, which uses the reflection response only, the proposed 3D extension requires, in addition to the reflection response, independent information about the first arrivals. Our derivation is based on physical arguments and still needs a mathematical justification. Furthermore, it remains to be investigated how well the method performs in case of finite acquisition apertures, triplications in the direct arriving wave front, head-waves, diving waves, fine layering, etc. Nevertheless, for those configurations for which 3D wave field reconstruction from reflection data is possible, the potential applications are fascinating. We indicated how the method could be extended to account for internal multiples in prestack migration. With a 1D example we showed that we can image the reflectors with correct amplitudes, free of internal multiple ghosts, without requiring any prior information about the medium. We expect that the proposed 3D method will be comparably stable as the 1D method. Errors in the estimated first arrivals will cause defocusing and mispositioning (as in standard migration), but we expect that they will not affect the handling of the internal multiples.

ACKNOWLEDGEMENT

We would like to thank Evert Slob for the fruitful discussions.

References

Bakulin, A. and R. Calvert, 2006, The virtual source method: Theory and case study: Geophysics, **71**, SI139–SI150.

Berkhout, A. J., 1997, Pushing the limits of seismic imaging. Part II. Integration of prestack migration, velocity estimation and AVO analysis: Geophysics, **62**, 954–969.

Broggini, F., R. Snieder, and K. Wapenaar, 2011, Connection of scattering principles: focusing the wavefield without source or receiver: 81rst Annual International Meeting, Expanded Abstracts, this issue.

Mehta, K., A. Bakulin, J. Sheiman, R. Calvert, and R. Snieder, 2007, Improving the virtual source method by wavefield separation: Geophysics, **72**, V79–V86.

Rose, J. H., 2002, 'Single-sided' autofocusing of sound in layered materials: Inverse Problems, **18**, 1923–1934.

Snieder, R., K. Wapenaar, and K. Larner, 2006, Spurious multiples in seismic interferometry of primaries: Geophysics, **71**, SI111–SI124.

Verschuur, D. J., A. J. Berkhout, and C. P. A. Wapenaar, 1992, Adaptive surface-related multiple elimination: Geophysics, **57**, 1166–1177.

Wapenaar, K. and J. van der Neut, 2010, A representation for Green's function retrieval by multidimensional deconvolution: Journal of the Acoustical Society of America, **128**, EL366–EL371.